Energy Reports 15 (2026) 109348

Contents lists available at ScienceDirect

Energy Reports

journal homepage: www.elsevier.com/locate/egyr

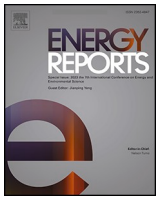

Research paper

Scalable self-powered electrochromic smart windows using gel electrolytes

Md Halim Hossain [a,b,c,1,2,3,5], Chil Seong Ah [b,5], Hojun Ryu [a,b,*,5,4]

[a] University of Science and Technology (UST), Daejeon 34113, Republic of Korea
[b] Advanced Materials and Device Engineering, Electronics and Telecommunication Research Institute (ETRI), Daejeon 34129, Republic of Korea
[c] Nanoscience and Technology, Korea Institute of Science and Technology (KIST), Seoul 02792, Republic of Korea

ARTICLE INFO

Keywords:
Gel electrolyte
Polyvinyl alcohol (PVA)
Self-powered
Electrochromic window
Energy-efficient building component

ABSTRACT

Self-powered electrochromic smart windows have emerged as essential components in sustainable building technologies. This study presents an innovative approach using polyvinyl alcohol (PVA) based gel electrolytes, which addresses limitations in conventional liquid electrolyte systems, including leakage and durability issues. A roll-to-roll slot-die coating process was successfully implemented, enabling uniform film deposition and scalability for large architectural applications. The fabricated 40 mm × 40 mm device exhibited a superior optical modulation of 58 ± 2.6% at a wavelength of 600 nm, a rapid coloration time of approximately 1.5 min, and a spontaneous bleaching time of around 8 min, outperforming many existing self-powered electrochromic devices. The optimized gel composition (40% PVA, 0.5 M $AlCl_3$, 80 mM APS) demonstrated high ionic conductivity (7.44 ± 0.17 mS/cm at 21°C), excellent optical transparency (90 ± 2%), and strong mechanical stability. Furthermore, a large-area device of 300 cm^2 was fabricated and visually confirmed to operate with improved coloration response using a three-sided aluminum counter electrode, reducing coloration time from around 10 min to under 4 min. These results are promising for the practical deployment of scalable, energy-efficient, and self-powered electrochromic smart windows.

1. Introduction

In modern architecture and sustainable design, the integration of smart technologies has emerged as a pivotal frontier, providing solutions that balance energy efficiency, comfort, and aesthetic appeal (Han et al., 2010; Strengers et al., 2020). Among these technologies, electrochromic devices (ECDs) stand out as versatile tools capable of dynamically modulating light transmission properties in response to external stimuli, revolutionizing the functionality and efficiency of windows and glass facades (Chavan et al., 2024; Han et al., 2023). Electrochromic windows provide multiple benefits, including dynamic control over daylight penetration and solar heat gain. These windows reduce the need for artificial lighting and HVAC (Heating, Ventilation, and Air Conditioning) systems, thereby lowering energy consumption and greenhouse gas emissions (Detsi et al., 2024; Gadgil et al., 2024; Rezaei et al., 2017). They also enhance occupant comfort by reducing glare and regulating indoor temperatures, creating a conducive environment for productivity and well-being (Cannavale et al., 2020).

Electrochromism, characterized by reversible color changes induced by an electric field, forms the cornerstone of electrochromic devices (Niklasson and Granqvist, 2007; Wang et al., 2024). These devices typically consist of transparent conductive electrodes separated by an electrolyte layer, with electrochromic materials deposited them (Granqvist, 2005). When a voltage is applied, ions shuttle between the electrodes, causing the electrochromic material to undergo oxidation or reduction, which alters its optical properties, such as light transmission and absorption (Gellings and Bouwmeester, 1997). The performance of electrochromic devices depends significantly on the type of electrochromic materials used. Factors such as coloration efficiency, switching speed, cycling stability, and optical contrast are influenced by the

* Correspondence to: University of Science and Technology (UST), 217 Gajeong-ro, Yuseong-gu, Daejeon, 34113, Republic of Korea.
E-mail addresses: hossain@ust.ac.kr (M.H. Hossain), acs@etri.re.kr (C.S. Ah), hjryu@etri.re.kr (H. Ryu).
[1] ORCID: https://orcid.org/0000-0002-7123-0183
[2] University of Science and Technology (UST), 217 Gajeong-ro, Yuseong-gu, Daejeon, 34113, Republic of Korea
[3] Korea Institute of Science and Technology (KIST), 5, Hwarang-ro 14-gil Seongbuk-gu, Seoul, 02792, Republic of Korea
[5] Electronics and Telecommunications Research Institute, 218 Gajeong-ro, Yuseong-gu, Daejeon, 34129, Republic of Korea
[4] ORCID: https://orcid.org/0000-0002-0555-5369

https://doi.org/10.1016/j.egyr.2026.109348
Received 7 October 2024; Received in revised form 20 October 2025; Accepted 15 April 2026
Available online 29 April 2026

material's intrinsic properties and structure. For example, tungsten trioxide (WO_3) nanorods with carved structures exhibit superior switching speeds of 5 s for coloration and 15 s for bleaching at 600 nm due to their pseudocapacitive behavior, whereas solid nanorods offer enhanced modulation contrast by accommodating a higher charge density (Zhai et al., 2022). Similarly, viologen-based organic electrochromic materials demonstrate high coloration efficiency (up to 142 cm^2 C^{-1}) and rapid switching times of 6 s for coloration and 9 s for bleaching, making them well-suited for dynamic display applications (Yang et al., 2020). While conventional electrochromic windows have showcased remarkable potential, their widespread adoption has been hindered by several inherent limitations, including the reliance on external power sources for operation, complex fabrication processes, and inadequate scalability (Zeng et al., 2019). Addressing these challenges, the paradigm of self-powered (SP) electrochromic windows has emerged as a transformative solution, offering autonomy and sustainability by harnessing ambient energy sources for operation, thereby circumventing the need for external power supplies (Dyer et al., 2014; Yang et al., 2012; Zheng et al., 2024). Recent advances in electrochromic technology have focused on achieving self-powering capabilities and enhancing scalability for commercial use. The first dual-function smart window was developed by using Prussian blue as the electrochromic material in a potassium chloride (KCl) aqueous electrolyte (Wang et al., 2014).

While liquid electrolytes have paved the way for initial developments in self-powered electrochromic devices because of their higher ionic conductivity, their inherent drawbacks limit their practical applications (Hossain et al., 2024; Hossain and Ryu, 2023; Q. Ma et al., 2023; Wang et al., 2014; Zhai et al., 2019). For example, reported SP ECD with an open upper part to introduce air O_2 (Wang et al., 2014) or Mg∼PB∼MnO_2 self-powered ECD using Li liquid electrolytes (Q. Ma et al., 2023) are not suitable for real-life applications. One of the primary disadvantages of liquid electrolytes is their tendency to leak, leading to device failure and safety hazards (Alesanco et al., 2018; Brazier et al., 2007). Furthermore, liquid electrolytes pose significant challenges in terms of stability and durability, over time, these electrolytes are prone to evaporation and degradation. In contrast, gel-based electrolytes offer a compelling alternative with several advantages. Gel polymer electrolytes (GPEs) offer a solid-like structure while retaining the high ionic conductivity of liquids, making them ideal for applications in electrochromic smart windows, as demonstrated by a PVA/H_2SO_4/Glutaraldehyde/H_2O gel electrolyte, which exhibited an ionic conductivity of 82 mS cm^{-1} and significantly enhanced electrochemical performance by enabling a large areal capacitance of 488 mF cm^{-2} (Alipoori et al., 2020). This hybrid nature helps mitigate leakage issues, as the gel matrix confines the electrolyte within a stable and flexible polymer network. Another limitation of liquid electrolytes is scalability, whereas employing gel electrolytes enables easier scaling of electrochromic smart windows, making them more feasible for practical applications (Lee et al., 2020; Primiceri et al., 2022; Santiago et al., 2019). For instance, UV-curable gel polymer electrolytes, such as those based on PMMA and $LiClO_4$ in propylene carbonate, have demonstrated excellent scalability, enabling the fabrication of large-area electrochromic devices up to 100 cm^2 with high optical contrast ($\Delta T \approx 51\%$ at 550 nm) and fast switching times (1.5 s for bleaching and 2 s for coloration) while maintaining operational stability over 115,000 cycles (Primiceri et al., 2022). By encapsulating electrochromic materials within a gel matrix, these electrolytes facilitate efficient ion transport while ensuring mechanical robustness, thus enabling seamless integration into large-scale manufacturing processes.

In this study, we address the gap in scalable, self-powered EC devices by developing a gel-based electrochromic system with high ionic conductivity, improved bleaching speed, and large-area compatibility. The proposed approach integrates a novel PVA-APS electrolyte formulation with a roll-to-roll process and counter electrode redesign, contributing a practical route toward industrial EC smart windows.

2. Experimental section

2.1. Materials

We used ITO PET film with a thickness of 188 μm (including a 50 μm protective film and 125 μm PET layer), a width of 0.60 m, and a length of 150 m as the transparent conductive electrode due to its flexibility, high optical transparency (∼92%), and low sheet resistance (35 Ω/cm^2), which are crucial for achieving high transmittance modulation and efficient ion transport. The WO_3 precursor solution (Adcro Co. Ltd, South Korea), which had a milky-green appearance, contained 15.7% solid content and a viscosity of 11 cp at 25°C. It was chosen as the electrochromic materials due to its well-documented properties, including high stability and reversible optical switching capabilities. Additionally, eight-folded aluminum foil with a thickness of approximately 0.6 mm was used as a counter electrode. Its flexibility aligns with the intention to produce a durable and scalable device. Potassium chloride (reagent grade, 99%) and ammonium persulfate (reagent grade, 98%) were both obtained from Sigma-Aldrich. We also used Polyvinyl alcohol (PVA), which was 87–90% hydrolyzed with an average molecular weight of 30,000–70,000, sourced from Sigma-Aldrich.

2.2. Preparation of gel electrolyte

The PVA-based gel electrolyte, with solid content of 24%, ionic conductivity of 7.44 ± 0.17 mS cm^{-1} (21 °C), and viscosity of 1.825 ± 0.06 Pa.S (21 °C, 13 rpm, 88% torque) was prepared at ambient laboratory conditions with a recorded temperature of approximately 21°C and relative humidity around 40–50%. The gel formulation consisted of 20 mL of deionized water, 40% PVA, 0.5 M aluminum chloride hexahydrate, and 80 mM ammonium persulfate. PVA powder was gradually added to the solution and stirred at 400 rpm for 3 h at room temperature without applying heat. This PVA gel electrolyte exhibits exceptional clarity, outstanding resilience to environmental conditions, robust ion conductivity, a straightforward preparation process, and cost-effectiveness.

2.3. Fabrication of electrochromic device

Before depositing the wet WO_3, the ITO film underwent plasma treatment in a controlled chamber at a pressure of 1.5 mTorr to enhance adhesion. The conditions for the treatment were 800 W power, 25 slm (Standard Liter per Minute) Ar, and 20 sccm (Standard Cubic Centimeter per Minute) O_2. Then, the WO_3 preparatory solution was shaken for 30 min. Continuous and scalable manufacturing was made possible by using a roll-to-roll (R2R) slot-die wet coating approach at a line speed of four meters per minute. After stabilization for two minutes at 130 ° Celsius, the wet-coated layer was dried, yielding a hardened WO_3 film that measured around 550 nm. Next, the electrode was cut into 60 mm by 60 mm sections to make the working electrode.

The counter electrode utilized was an aluminum strip measuring 70 × 6 mm^2. Subsequently, the complete assembly of the electrochromic device involved combining both the working and counter electrodes using PET film and acrylic double-sided adhesive tape. The gel electrolyte was sandwiched between the WO_3 working electrode and the PET film to complete the device assembly. Fig. 1 demonstrates the schematic illustration of the gel electrolyte-based EC smart window fabrication process.

2.4. Performance measurement techniques

To ensure accurate and relevant data, each performance measurement technique was carefully selected based on its suitability to the study's objectives. The following justifications clarify the device specifications and the rationale behind choosing each method:

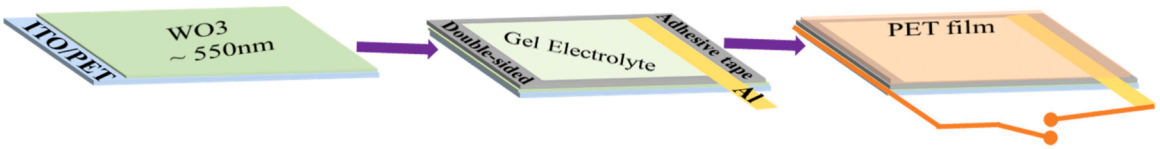

Fig. 1. Simple schematic diagram of gel electrolyte-based EC smart window fabrication.

i) Optical Properties Measurement (USB2000 + Spectrometer and DH-2000-BAL Light Source, Ocean Optics, Inc., USA):
   The spectrometer was chosen for its ability to provide high-resolution spectral data in the UV-Vis-NIR range, crucial for evaluating the transmittance modulation of the electrochromic device. Given that the device's primary function is to modulate light transmission, this tool was ideal for quantifying optical contrast and switching behavior at relevant wavelengths (e.g., 600 nm).
ii) Electrochemical Properties Measurement (CHI1030 Multi-potentiostat, CH Instruments, Inc., USA):
   The electrochemical workstation was selected for its high current sensitivity, enabling precise characterization of the device's anodic and cathodic peaks during cyclic voltammetry. These measurements provided valuable insights into the redox processes governing coloration and bleaching, ensuring a thorough understanding of the device's switching dynamics and stability.
iii) Ionic Conductivity Measurement (Orion Star A212 Conductivity Meter, Thermo Scientific):
   Accurately measuring ionic conductivity was essential for evaluating the efficiency of ion transport within the gel electrolyte. The tool's high precision ensured reliable data, which was crucial for correlating conductivity with switching performance.
iv) Viscosity Measurement (DV3THBCJ0 Rheometer, USA):

The rheometer was used to measure the gel electrolyte's viscosity. Optimal viscosity ensures efficient ion mobility for fast switching and prevents leakage, and maintains structural integrity.

All key measurements (e.g., transmittance, optical modulation, ionic conductivity, and viscosity) were conducted three times to ensure consistency. Reported values in the Results and Discussion represent the average of at least three independent measurements. In all cases, the variation was $< 5\%$ over three independent tests.

2.5. Experimental stability and repeatability control

To guarantee consistent and replicable outcomes, various measurements were implemented during the experimental procedure. All electrochemical and optical measurements were conducted under controlled ambient conditions (21 ± 1 °C, 40–50% relative humidity). Instruments such as the UV-Vis spectrophotometer, digital ionic conductivity meter, and rheometer were calibrated before each measurement session. Electrolyte preparation procedures (e.g., heating time, stirring speed, and cooling conditions) were strictly maintained for all batches. Gel layers were cast using identical thickness and area dimensions to eliminate device-to-device variability. For switching performance evaluation, each device was cycled a minimum of 25 times to assess reproducibility and degradation, with stable optical modulation and response time observed. Additionally, device edges were sealed using transparent adhesive to prevent moisture loss and contamination during measurements. For large-area samples, the three-sided counter electrode design helped reduce spatial inhomogeneities and maintained consistent ion transport across the active area.

3. Results and discussion

In a 0.5 M $AlCl_3$ aqueous electrolyte, the WO_3-based EC smart window functioned as a self-powered device. This behavior resulted from the potential gradient between Al and WO_3 electrodes. When connected, the open-circuit output voltage between the electrodes acts as an external power source. This drives the transparent WO_3 EC window into its colored state. Fig. 2a shows that while coloration is rapid, the spontaneous bleaching process is relatively slow. To increase the bleaching rate, we added ammonium persulfate bleaching compound with $AlCl_3$ electrolyte.

Fig. 2b illustrates the effect of varying Ammonium Persulfate (APS) concentrations on transmittance modulation and bleaching rate. The data reveal that increasing APS concentration enhances the bleaching rate but decreases the transmittance modulation. These results highlight the importance of optimizing APS concentration. Controlled levels improve bleaching speed without severely compromising optical contrast, enhancing overall device efficiency. Considering both a higher range of transmittance modulation and a higher bleaching rate, for further experiments, we used 40 mM APS as the optimized concentration with 0.5 M $AlCl_3$ electrolyte.

However, the use of liquid electrolytes faces various disadvantages, such as electrolyte leakage, performance degradation with temperature variation, and complexity with large-scale fabrications. To overcome these drawbacks, we transformed our electrolytes into a gel using water-soluble PVA (Polyvinyl Alcohol) powder. Fig. 3a shows that the gel-based SP EC window demonstrates slightly lower performance compared to liquid electrolytes. This is mainly due to the decline of ionic conductivity of the gel electrolytes (Sekhon, 2003). The selection of PVA concentration was guided by the need to balance ionic conductivity and optical transparency, two critical parameters influencing the performance of electrochromic devices. Lower PVA concentrations, such as 30%, resulted in higher ionic conductivity (6.728 mS/cm at 21°C) but compromised mechanical integrity, leading to potential leakage and instability over time. On the other hand, increasing the PVA content to 40% enhanced the mechanical robustness and stability of the gel electrolyte, but slightly reduced ionic conductivity to 4.946 mS/cm at 21°C (Fig. 3c). This trade-off directly impacts the coloration and bleaching dynamics of the device. Higher ionic conductivity allows for faster ion transport, leading to quicker electrochromic switching. Very low PVA concentrations weaken the gel structures, making it prone to dehydration and phase separation, which degrades long-term stability. In contrast, while higher PVA concentrations reduce ionic mobility slightly, they ensure a more stable electrolyte matrix that prevents leakage and enhances device longevity.

Another important consideration was the effect of PVA concentration on transparency. While lower PVA levels produced clearer electrolytes, the increased water content contributed to faster evaporation and reduced lifespan. Conversely, at 40% PVA, the electrolyte retained sufficient transparency (>90%) while providing the necessary mechanical strength and longevity for large-scale applications.

The selected 40% PVA formulation represents an optimal balance, ensuring adequate ionic conductivity for efficient switching while maintaining transparency and structural integrity. The 30% and 40% PVA electrolytes viscosity were 1.314 Pa.S and 1.791 Pa.S respectively at 21°C, 13 rpm, and 88% torque. Again, to increase the bleaching rate of the gel-based ECD, we need to further optimize the APS concentration. From Fig. 3b, we concluded that 80 mM APS is the optimal concentration for the gel PVA gel electrolyte. Now the gel electrolyte demonstrates moderate ionic conductivity (7.44 ± 0.17 mS/cm), viscosity (1.825 ± 0.06 Pa.S), and transparency ($90 \pm 2\%$) comparable to the other gel

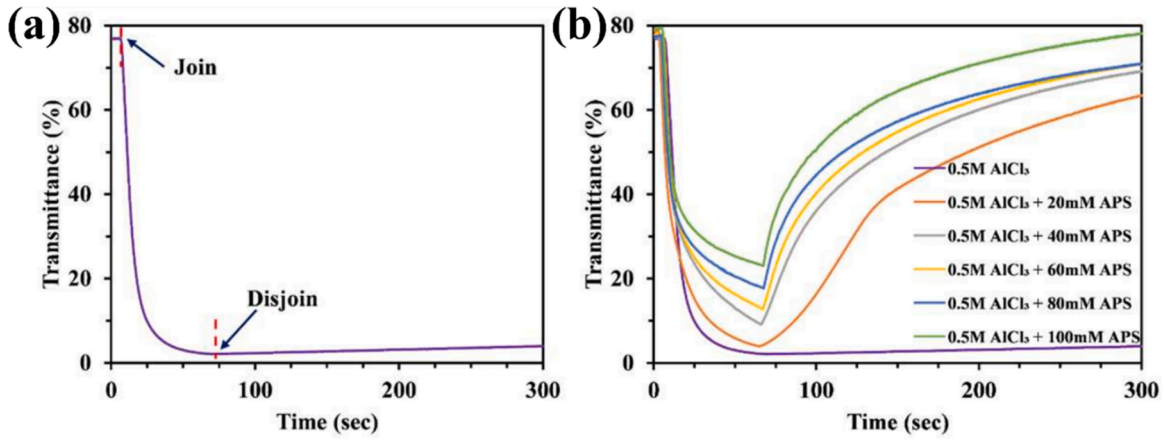

Fig. 2. (a) Coloration and bleaching process of the WO_3 SP EC window in 0.5 M $AlCl_3$ aqueous electrolyte, (b) addition and optimization of APS (Ammonium persulfate) concentration for higher transmittance modulation and bleaching rate.

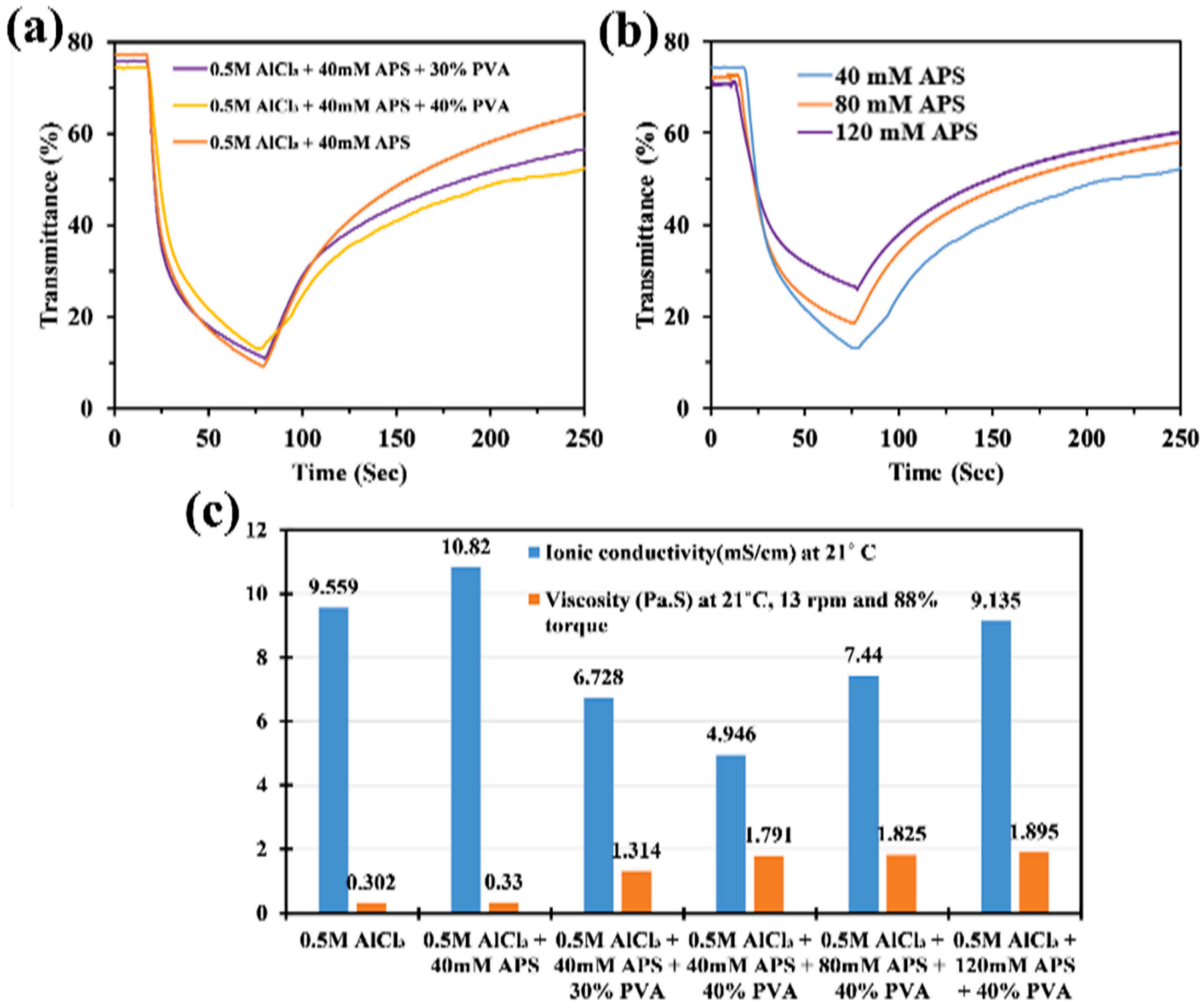

Fig. 3. (a) Variation of coloration and bleaching performance with the gel formation using different percentages of PVA concentrations; (b) further bleaching property improvement for 40% PVA gel electrolyte-based self-powered ECD with the addition of Ammonium persulfate (APS) concentrations; and (c) variation of ionic conductivity and viscosity of electrolytes with different conditions.

electrolyte-based EC devices (Ah et al., 2021).

Fig. 4 shows the bleached and colored states of the gel-electrolyte-based WO_3 self-powered EC smart window. When the WO_3 working electrode and the Al counter electrode are connected, the transparent WO_3 electrode changes to blue. We connected the two electrodes for 3 min, and the measured in-situ transmittance spectra indicate the respective transmittance change (Fig. 5a). At 600 nm wavelength, the device shows approximately 58% transmittance modulation, which is comparatively higher than some other self-powered devices (Huang et al., 2016, 2012; Wang et al., 2021). According to Fig. 5c, the device shows fast coloration in only 1.5 ± 0.2 min. Here, the color switching time is defined as the duration required to achieve 90% of the final transmittance change.(Gu et al., 2018) Reversibly, to regain the transparent state, we disconnected the two electrodes for 13 min (Fig. 5b). The spontaneous bleaching time was measured to be $\sim$ Tb $= 8 \pm 0.7$ min (Fig. 5d), indicating the time required for the device to revert to its bleached state without external power - a key metric for self-powered EC systems.

Several measures can be used to lessen bleaching time in the future. Using stronger oxidising agents, such as hydrogen peroxide (H_2O_2) or ferric ions (Fe^{3+}), might accelerate oxidation reactions inside the gel matrix, resulting in a spontaneous reversion to the bleached state (Kong et al., 2022; Ma et al., 2020). Furthermore, altering the gel electrolyte by combining PVA and polyethylene glycol (PEG) or adding ionic liquids has been demonstrated to improve ionic mobility, which is required for efficient bleaching (Deng et al., 2023; Garino et al., 2013). Nanostructured WO_3 films, including mesoporous or nanorod morphologies, can minimise ion diffusion lengths and accelerate switching (Huang et al., 2023; Zhao et al., 2025). Finally, thermal or UV-assisted bleaching technologies, which use ambient energy to facilitate spontaneous recovery, provide another option for speeding up bleaching without requiring additional power (Huang et al., 2022; Yang et al., 2025).

In comparison to recent literature, our device demonstrates a strong balance of electrochromic performance parameters. Aloe vera gel electrolyte-based self-powered electrochromic windows exhibited a spontaneous recovery time exceeding 31 min (Nanda et al., 2018). PAM/LiCl gel-based NiHCF/PB device demonstrated 40% optical modulation, 8.5 s bleaching time, and 21.5 min coloration time (Xue et al., 2023). Though the bleaching time is fast, the coloration time is very slow. Similarly, an $Al(ClO_4)_3$-based self-powered electrochromic window with a recovery time of 29.92 min (Ge et al., 2025). In comparison, the PVA-based gel electrolyte developed in this study achieved a significantly faster spontaneous bleaching time of 8 min. This demonstrates a significant improvement in recovery efficiency, highlighting the superior ionic transport and stability of the PVA-based electrolyte formulation. Besides, our device performance also surpasses some previously reported liquid electrolyte-based SP windows (Huang et al., 2016, 2012; Wang et al., 2014). The details comparison is presented in Table 1. Further, the reversibility and repeatability of our device were measured by connecting and disconnecting the Al wire for 25 cycles, which demonstrates the excellent performance of our device over time (Fig. 6).

The coloration and bleaching mechanism of this device can be explained by the following equations-

Coloration

$$\text{Anode: } Al = Al^{3+} + 3e^-$$

$$\text{Cathode: } WO_3 + Al^{3+} + 3e^- = AlWO_3$$

Bleaching:

$$\text{Anode: } AlWO_3 - e^- = WO_3 + Al^{3+}$$

$$\text{Cathode: } S_2O_8^{2-} + 2e^- = 2SO_4^{2-}$$

We performed cyclic voltammetry on the WO_3 electrochromic device using a two-electrode configuration. The aluminum (Al) electrode served as both the counter and reference. The results revealed redox behavior essential to the device's switching mechanism. The voltammogram showcases distinct anodic and cathodic peaks, indicative of the oxidation and reduction processes associated with ion intercalation and de-intercalation within the WO_3 matrix (Fig. 7a). The anodic peak occurs at approximately 0.35 V with a peak current of 0.4 mA, while the cathodic peak is observed at around 0.7 V with a peak current of −1.5 mA. The observed hysteresis loop suggests capacitive characteristics and energy storage capabilities, with the area enclosed by the loop reflecting the efficiency of these processes. Symmetry in the peaks denotes balanced redox reactions, though the potential influence of the Al electrode's dual role should be considered, as it may introduce additional electrochemical activities.

The battery characteristics of our self-powered electrochromic device were investigated by measuring the output voltage changes when the two electrodes of the device were alternately connected and

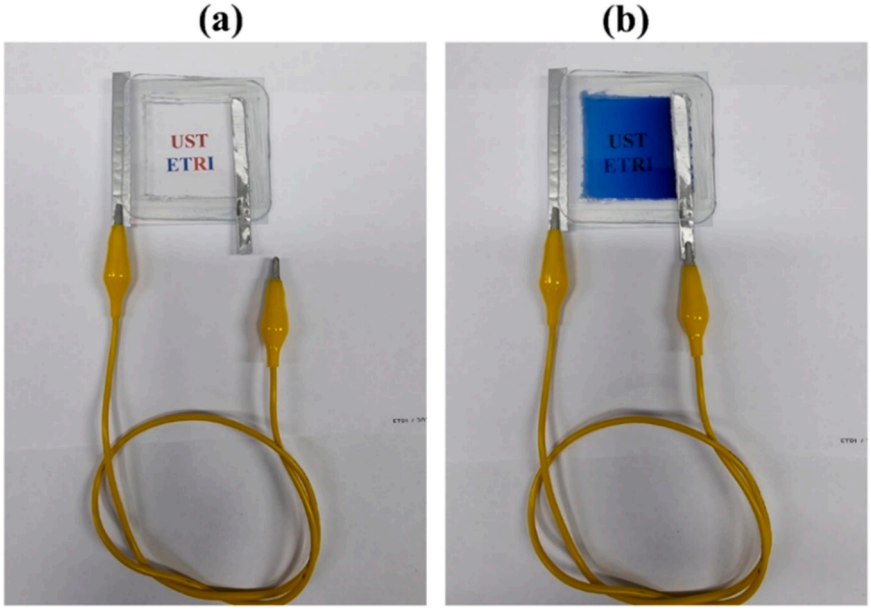

Fig. 4. (a) Bleached and (b) colored states of 0.5 M $AlCl_3$ + 80 mM APS + 40% PVA gel-electrolyte-based WO_3 self-powered EC smart window.

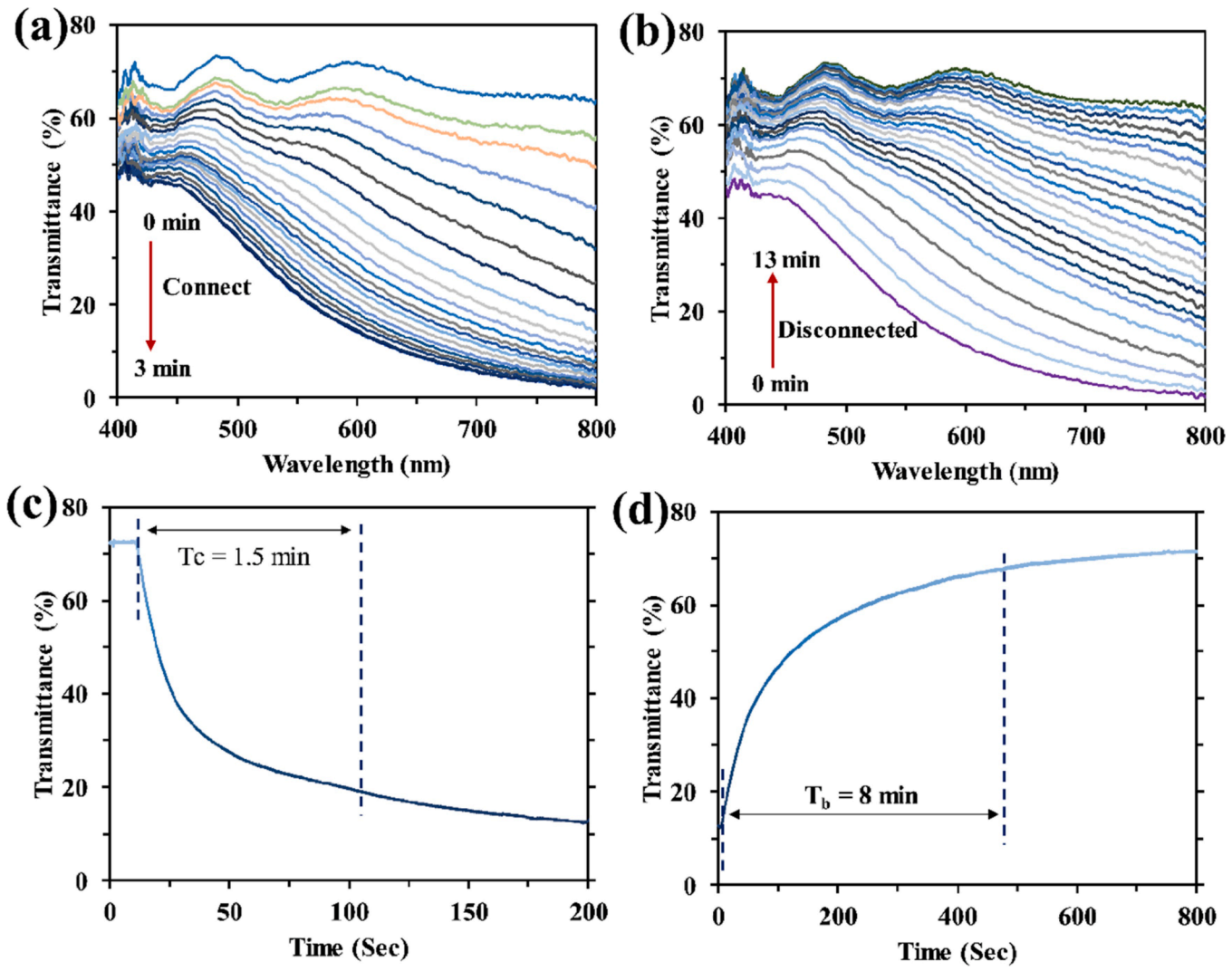

Fig. 5. (a & b) Transmittance spectra in the coloration and bleaching process upon connection and disconnection of Al and WO_3 electrodes in the PVA gel-electrolyte; (c & d) percentage transmittance change with time in the coloration and bleaching process, demonstrating approximately 1.5 min and 8 min coloration and bleaching time, respectively; and (e).

Table 1
Comparison of this study with other gel based self-power ECD.

Gel Type	Optical Modulation	Coloration Time	Bleaching Time	Ionic Conductivity (mS/cm)	Ref.
PVA Gel	58% @ 600 nm	1.5 min	8 min	7.44	This work
Aloe vera gel	~48% @ 600 nm	58 s	> 31 min	Not reported	(Nanda et al., 2018)
PAM/LiCl gel	< 40% @ 400 nm	21.5 min	8.5 s	Not reported	(Xue et al., 2023)
$Al(ClO_4)_3$ hydrogel	42.5% @ 550 nm	9.62 s	29.92 min	10.1	(Ge et al., 2025)

disconnected (Fig. 7b). Initially, the 40 × 40 mm^2 active area device provides approximately 1.07 ± 0.02 V stable open circuit output voltage. When the electrodes were connected, the output voltage rapidly dropped to 0.02, and the device went into a colored state by implementing open circuit voltage as an external voltage. Upon disconnecting the electrodes, the device starts to recover its initial voltage. While a similar reported device could recover 65% open-circuit voltage (Voc) after 1 h self-charging, our device recovers more than 50% within 60 s (D. Ma et al., 2023). This transition between the connected and disconnected states was consistently reproducible.

To understand the large-scale fabrication of the SP smart window, we fabricated a 20 cm × 15 cm device. The bleached and colored state of this wide device is shown in Fig. 8. For large-scale devices, we observed that the coloration process started from the Al electrode and took a long time for full coloration, also the nearest areas of the Al anode got darker blue colored than the furthest areas (Fig. 8b). This major challenge encountered was due to the uneven distribution of ions across the active area, leading to inconsistencies in coloration. As the device size increased from 16 cm^2 to 300 cm^2, it became evident that ion transport was not uniform, resulting in delayed coloration in regions further from the aluminum counter electrode. This non-uniformity arose because ions needed to travel greater distances, causing variations in electrochemical reactions. The areas closest to the counter electrode underwent faster and more intense coloration, while those further away lagged behind. Additionally, edge effects contributed to slower response times at the periphery of the device, reducing overall performance consistency. To address this issue, we designed a three-sided aluminum counter electrode configuration. This modification allowed for ion transport from

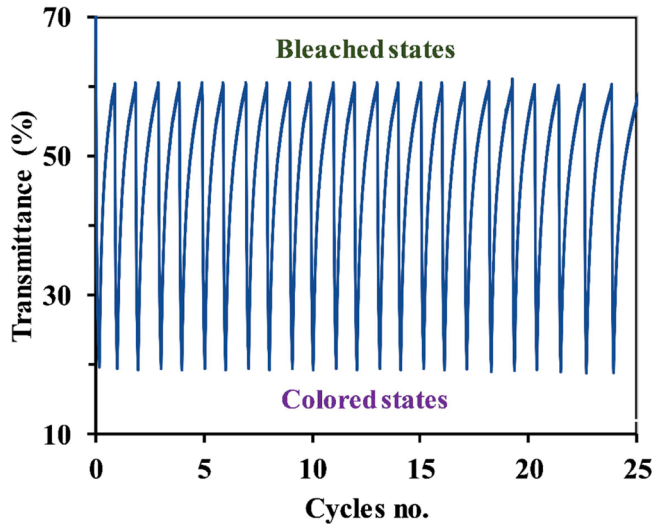

Fig. 6. Repeated coloration and bleaching over 25 cycles at 600 nm wavelength.

multiple directions, ensuring a more uniform potential gradient and minimizing coloration delay. The introduction of additional electrode contact points facilitated more homogeneous ion migration, thereby significantly improving the visual uniformity and response time of the device (Fig. 8c). This solution significantly reduced the coloration time, before implementing the three-sided electrode configuration, the device required approximately 10 min to fully transition to the colored state across the entire active area. With the optimized design, this time was reduced to less than 4 min. Electrochemical impedance spectroscopy (EIS) measurements further validated this improvement, demonstrating a reduction in ion diffusion resistance by approximately 35%. Although large-area operation was visually confirmed, further quantitative performance validation at scale is necessary. The proposed three-sided electrode design demonstrates promising potential but requires additional optimization for commercial application. Further, as we used an ITO-PET flexible film substrate instead of a rigid glass substrate and folded Al foil for the flexible anode, our device demonstrates a high range of flexibility. Fig. 8d exhibits the flexible characteristics of our fabricated PVA gel-electrolyte-based WO_3 EC smart window.

This work focused on the proof-of-concept demonstration of a self-powered electrochromic smart window with a PVA-based gel electrolyte. While promising results were obtained, numerous constraints remained: (i) Quantitative data on large-area devices were limited; (ii) the parameter space for material optimisation was constrained; (iii) no simulation or modelling was carried out; and (iv) no environmental or long-term durability testing were performed. These features will be investigated further in the future to improve their practical use.

4. Conclusion

In conclusion, this study addresses the challenge of scaling self-powered electrochromic smart windows by introducing a 40% PVA-based gel electrolyte that enhances stability, prevents leakage, improves durability, and enables large-area fabrication. Our experimental results underscore the superior performance of these gel electrolytes. The device produces a 1.07 V open circuit output voltage, overcoming external power dependency. The devices exhibited fast coloration (1.5 min) and reversible bleaching (8 min), demonstrating robust operational efficiency. The demonstrated scalability of our device from 16 cm^2 to 300 cm^2 further supports the feasibility of large-scale production for commercial applications as smart windows in zero-energy buildings. We have successfully addressed key challenges in the large-scale production of self-powered electrochromic smart windows, particularly regarding ion distribution uniformity and material stability. The implementation of a three-sided aluminum counter electrode significantly improved coloration response and uniformity. These advancements contribute to energy savings, enhanced occupant comfort, and pave the way for sustainable building designs with intelligent and efficient smart window technologies.

Future research may focus on further improving bleaching speed by incorporating advanced oxidizing agents, hybrid electrolytes, and nanostructured WO_3 films to minimize ion diffusion length. Alternative counter electrode designs (such as mesh or grid patterns) could also be investigated to ensure uniform ion transport in large-area applications. Simulation and modeling of ion dynamics in large devices can guide design optimization. Moreover, evaluating long-term durability under varying environmental conditions (UV exposure, temperature, humidity) will be critical for real-world applications. With proper encapsulation and scaling procedures, this gel-based, self-powered electrochromic platform can be integrated into energy-efficient buildings, flexible electronics, and smart building exteriors.

CRediT authorship contribution statement

Hojun Ryu: Writing – review & editing, Validation, Project administration, Investigation. **Md Halim Hossain:** Writing – original draft, Visualization, Methodology, Data curation, Conceptualization. **Chil**

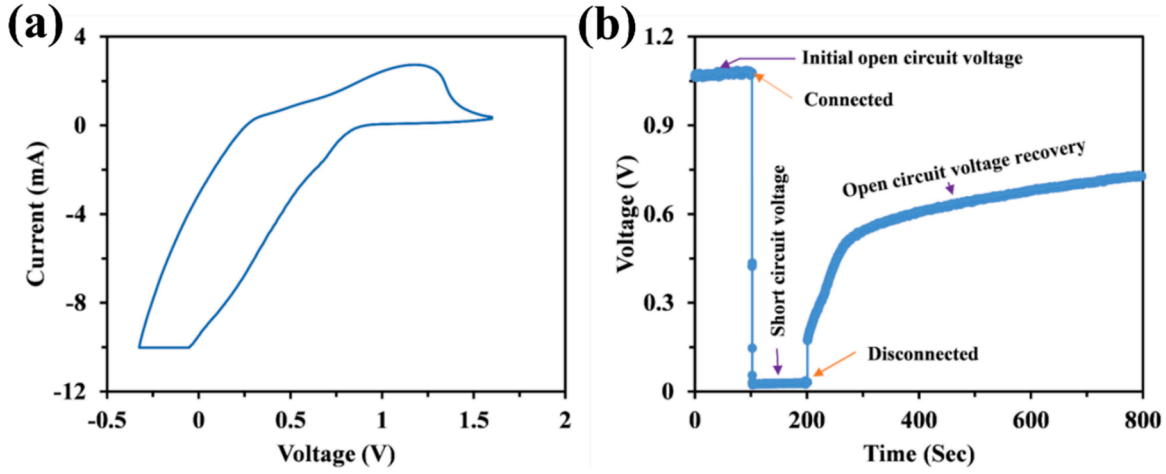

Fig. 7. (a) Cyclic voltammogram of the self-powered EC window at a scan rate of 100 mV/s using two electrode configurations; and (b) self-powered working mechanism, initial open circuit voltage, short circuit voltage, and voltage recovery process.

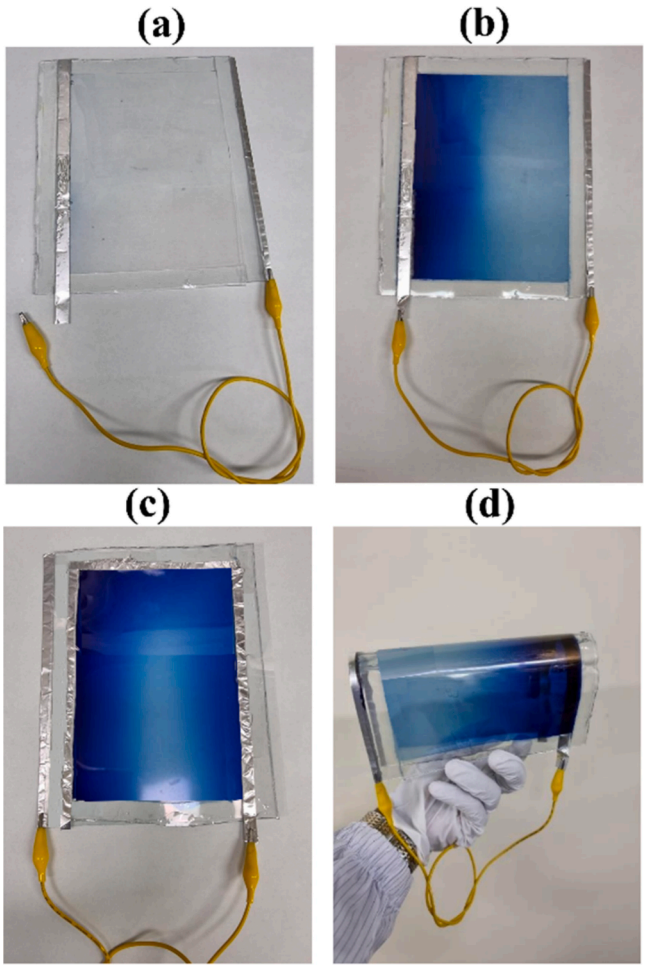

Fig. 8. Large-scale fabrication of PVA gel-electrolyte-based SP EC smart windows, (a) transparent state; (b) colored state; (c) improved colored state using 3 sides Al counter electrode; and (d) flexible characteristics of the fabricated EC window.

Seong Ah: Validation, Methodology, Investigation.

Declaration of Competing Interest

The authors declare no competing financial interests or personal relationships that influence the work reported in this manuscript.

Acknowledgements

This research was supported by the Korea Planning & Evaluation of Industrial Technology (KEIT) grant (20025884, the Development of international standards for the evaluation methods of wearable equipment in metaverse environment) and Electronics and Telecommunications Research Institute (ETRI) grant funded by the Korea government. (24ZH1200, The Development of the Technologies for ICT Materials, Components and Equipment).

Notes

The authors declare no competing financial interest.

Data Availability

Data will be made available on request.

References

Ah, C.S., Song, J., Kim, T.-Y., Han, J., Sung, C., Cho, D.-H., Cheon, S., Cho, S.M., Ryu, H., 2021. Long-lived electrochromic device with multilevel bistability based on portable film-type polymer electrolytes. Sol. Energy Mater. Sol. Cells 221, 110883. https://doi.org/10.1016/j.solmat.2020.110883.

Alesanco, Y., Viñuales, A., Rodriguez, J., Tena-Zaera, R., 2018. All-in-One Gel-Based Electrochromic Devices: Strengths and Recent Developments. Materials 11, 414. https://doi.org/10.3390/ma11030414.

Alipoori, S., Mazinani, S., Aboutalebi, S.H., Sharif, F., 2020. Review of PVA-based gel polymer electrolytes in flexible solid-state supercapacitors: Opportunities and challenges. J. Energy Storage 27, 101072. https://doi.org/10.1016/j.est.2019.101072.

Brazier, A., Appetecchi, G.B., Passerini, S., Surca Vuk, A., Orel, B., Donsanti, F., Decker, F., 2007. Ionic liquids in electrochromic devices. Electrochim. Acta 52, 4792–4797. https://doi.org/10.1016/j.electacta.2007.01.025.

Cannavale, A., Ayr, U., Fiorito, F., Martellotta, F., 2020. Smart electrochromic windows to enhance building energy efficiency and visual comfort. Energies 13, 1449. https://doi.org/10.3390/en13061449.

Chavan, P.V., Rathod, P.V., Kim, H., 2024. Sodium alginate grafted phase-changing electrolyte for energy-efficient thermochromic and electrochromic synergy with uniquely tunable optical states and simultaneous Vis-NIR modulation. Chem. Eng. J. 497, 154835. https://doi.org/10.1016/j.cej.2024.154835.

Deng, B., Zhu, Y., Wang, X., Zhu, J., Liu, Manyu, Liu, Mingqiang, He, Y., Zhu, C., Zhang, C., Meng, H., 2023. An ultrafast, energy-efficient electrochromic and thermochromic device for smart windows. Adv. Mater. 35, 2302685. https://doi.org/10.1002/adma.202302685.

Detsi, M., Atsonios, I., Mandilaras, I., Founti, M., 2024. Effect of smart glazing with electrochromic and thermochromic layers on building's energy efficiency and cost. Energy Build. 319, 114553. https://doi.org/10.1016/j.enbuild.2024.114553.

Dyer, A.L., Bulloch, R.H., Zhou, Y., Kippelen, B., Reynolds, J.R., Zhang, F., 2014. A vertically integrated solar-powered electrochromic window for energy efficient buildings. Adv. Mater. 26, 4895–4900. https://doi.org/10.1002/adma.201401400.

Gadgil, C., Ghosh, A., Bhattacharjee, A., Praveen, P.L., 2024. Electrically powered active smart windows. Sustainability 3, 100027. https://doi.org/10.1016/j.nxsust.2024.100027.

Garino, N., Zanarini, S., Bodoardo, S., Nair, J.R., Pereira, S., Pereira, L., Martins, R., Fortunato, E., Penazzi, N., 2013. Fast switching electrochromic devices containing optimized BEMA/PEGMA gel polymer electrolytes. Int. J. Electrochem. 2013, 1–10. https://doi.org/10.1155/2013/138753.

Ge, R., Xiao, X., Chen, L., Jiang, C., Nie, Y., Zhu, Y., Zhong, L., Xu, G., 2025. Anti-freezing polyacrylamide hydrogel electrolyte for rapid response self-powered electrochromic devices. J. Mater. Chem. A 10. 1039. D4TA08037H. https://doi.org/10.1039/D4TA08037H.

Gellings, P.J., Bouwmeester, H.J.M., 1997. The CRC handbook of solid state electrochemistry. CRC Press, Boca Raton, Fla.

Granqvist, C.G., 2005. Electrochromic devices. J. Eur. Ceram. Soc. 25, 2907–2912. https://doi.org/10.1016/j.jeurceramsoc.2005.03.162.

Gu, H., Guo, C., Zhang, S., Bi, L., Li, T., Sun, T., Liu, S., 2018. Highly efficient, near-infrared and visible light modulated electrochromic devices based on polyoxometalates and $W_{18}O_{49}$ nanowires. ACS Nano 12, 559–567. https://doi.org/10.1021/acsnano.7b07360.

Han, H.J., Jeon, Y.I., Lim, S.H., Kim, W.W., Chen, K., 2010. New developments in illumination, heating and cooling technologies for energy-efficient buildings. Energy 35, 2647–2653. https://doi.org/10.1016/j.energy.2009.05.020.

Han, S., Sun, Y., Wang, W., Xu, W., Wei, W., 2023. Optimal design method for electrochromic window split-pane configuration to enhance building energy efficiency. Renew. Energy 219, 119405. https://doi.org/10.1016/j.renene.2023.119405.

Hossain, M.H., Ryu, H., 2023. Development of a novel WO3 self-powered electrochromic window technology with a self-rechargeable battery application (ChromoVolt). Energy Rep. 10, 3780–3786. https://doi.org/10.1016/j.egyr.2023.10.046.

Hossain, M.H., Ah, C.S., Ryu, H., 2024. Investigation for a highly efficient self-powered electrochromic smart window for fast response and greater maximum transmittance modulation. ACS Appl. Electron. Mater. 6, 1514–1520. https://doi.org/10.1021/acsaelm.4c00010.

Huang, C., Hu, Z., Yi, Y.-Q.-Q., Chen, X., Wu, X., Su, W., Cui, Z., 2022. High performance printed organic electrochromic devices based on an optimized UV curable solid-state electrolyte. Nanoscale 14, 14122–14128. https://doi.org/10.1039/D2NR03209K.

Huang, L.-M., Hu, C.-W., Liu, H.-C., Hsu, C.-Y., Chen, C.-H., Ho, K.-C., 2012. Photovoltaic electrochromic device for solar cell module and self-powered smart glass applications. Sol. Energy Mater. Sol. Cells 99, 154–159. https://doi.org/10.1016/j.solmat.2011.03.036.

Huang, L.-M., Hu, C.-W., Peng, C.-Y., Su, C.-H., Ho, K.-C., 2016. Integration of polyelectrolyte based electrochromic material in printable photovoltaic electrochromic module. Sol. Energy Mater. Sol. Cells 145, 69–75. https://doi.org/10.1016/j.solmat.2015.05.011.

Huang, Q., Liang, Y., Cao, S., Yang, Z., 2023. Morphology-dependent near-infrared electrochromic properties of tungsten oxide. Coatings 13, 344. https://doi.org/10.3390/coatings13020344.

Kong, S., Zhang, G., Li, M., Yao, R., Guo, C., Ning, H., Zhang, J., Tao, R., Yan, H., Lu, X., 2022. Investigation of an electrochromic device based on ammonium metatungstate-Iron (II) chloride electrochromic liquid. Micromachines 13, 1345. https://doi.org/10.3390/mi13081345.

Lee, H.J., Lee, C., Song, J., Yun, Y.J., Jun, Y., Ah, C.S., 2020. Electrochromic devices based on ultraviolet-cured poly(methyl methacrylate) gel electrolytes and their

utilisation in smart window applications. J. Mater. Chem. C. 8, 8747–8754. https://doi.org/10.1039/D0TC00420K.
Ma, D., Yang, B., Wang, J., 2023. Boosting the self-recharging of polypyrrole/prussian blue electrochromic device by potential difference-driven alternative redox. ACS Appl. Mater. Interfaces 15, 56041–56048. https://doi.org/10.1021/acsami.3c14291.
Ma, Q., Zhang, H., Chen, J., Wu, W., Dong, S., 2020. Lithium-ion-assisted ultrafast charging double-electrode smart windows with energy storage and display applications. ACS Cent. Sci. 6, 2209–2216. https://doi.org/10.1021/acscentsci.0c01149.
Ma, Q., Chen, J., Zhang, H., Su, Y., Jiang, Y., Dong, S., 2023. Dual-function self-powered electrochromic batteries with energy storage and display enabled by potential difference. ACS Energy Lett. 8, 306–313. https://doi.org/10.1021/acsenergylett.2c02346.
Nanda, O., Gupta, N., Grover, R., Saxena, K., 2018. Self-powered electrochromic window using green electrolyte. AIP Adv. 8, 095117. https://doi.org/10.1063/1.5037454.
Niklasson, G.A., Granqvist, C.G., 2007. Electrochromics for smart windows: thin films of tungsten oxide and nickel oxide, and devices based on these. J. Mater. Chem. 17, 127–156. https://doi.org/10.1039/B612174H.
Primiceri, V., Pugliese, M., Prontera, C.T., Monteduro, A.G., Esposito, M., Maggiore, A., Cannavale, A., Giannuzzi, R., Gigli, G., Maiorano, V., 2022. Low-cost gel polymeric electrolytes for electrochromic applications. Sol. Energy Mater. Sol. Cells 240, 111657. https://doi.org/10.1016/j.solmat.2022.111657.
Rezaei, S.D., Shannigrahi, S., Ramakrishna, S., 2017. A review of conventional, advanced, and smart glazing technologies and materials for improving indoor environment. Sol. Energy Mater. Sol. Cells 159, 26–51. https://doi.org/10.1016/j.solmat.2016.08.026.
Santiago, S., Aller, M., Del Campo, F.J., Guirado, G., 2019. Screen-printable electrochromic polymer inks and ion gel electrolytes for the design of low-power, flexible electrochromic devices. Electroanalysis 31, 1664–1671. https://doi.org/10.1002/elan.201900154.
Sekhon, S.S., 2003. Conductivity behaviour of polymer gel electrolytes: Role of polymer. Bull. Mater. Sci. 26, 321–328. https://doi.org/10.1007/BF02707454.
Strengers, Y., Hazas, M., Nicholls, L., Kjeldskov, J., Skov, M.B., 2020. Pursuing pleasance: Interrogating energy-intensive visions for the smart home. Int. J. Hum. -Comput. Stud. 136, 102379. https://doi.org/10.1016/j.ijhcs.2019.102379.
Wang, J., Zhang, L., Yu, L., Jiao, Z., Xie, H., Lou, X.W., Wei Sun, X., 2014. A bi-functional device for self-powered electrochromic window and self-rechargeable transparent battery applications. Nat. Commun. 5, 4921. https://doi.org/10.1038/ncomms5921.
Wang, J., Wang, Z., Zhang, M., Huo, X., Guo, M., 2024. Toward next-generation smart windows: an in-depth analysis of dual-band electrochromic materials and devices. Adv. Opt. Mater. 12, 2302344. https://doi.org/10.1002/adom.202302344.
Wang, J.-L., Sheng, S.-Z., He, Z., Wang, R., Pan, Z., Zhao, H.-Y., Liu, J.-W., Yu, S.-H., 2021. Self-powered flexible electrochromic smart window. Nano Lett. 21, 9976–9982. https://doi.org/10.1021/acs.nanolett.1c03438.
Xue, W., Zhang, Y., Liu, F., Dou, Y., Yan, M., Wang, W., 2023. Self-Powered Flexible Multicolor Electrochromic Devices for Information Displays. Research 6, 0227. https://doi.org/10.34133/research.0227.
Yang, G., Zhang, Y.-M., Cai, Y., Yang, B., Gu, C., Zhang, S.X.-A., 2020. Advances in nanomaterials for electrochromic devices. Chem. Soc. Rev. 49, 8687–8720. https://doi.org/10.1039/D0CS00317D.
Yang, X., Zhu, G., Wang, S., Zhang, R., Lin, L., Wu, W., Wang, Z.L., 2012. A self-powered electrochromic device driven by a nanogenerator. Energy Environ. Sci. 5, 9462. https://doi.org/10.1039/c2ee23194h.
Yang, X., Duan, G., Liu, Y., Han, J., Han, X., Fu, H., He, S., Huang, Y., Zhang, K., Yin, Y., Jiang, S., 2025. Next-generation photochromic smart window: Wood-derived cellulose flexible composites integrated thermal insulation, UV -shielding, and anti-counterfeiting. InfoMat, e70049. https://doi.org/10.1002/inf2.70049.
Zeng, J., Wan, Z., Zhu, M., Ai, L., Liu, P., Deng, W., 2019. Flexible electrochromic energy-saving windows with fast switching and bistability based on a transparent solid-state electrolyte. Mater. Chem. Front 3, 2514–2520. https://doi.org/10.1039/C9QM00562E.
Zhai, Y., Li, Y., Zhang, H., Yu, D., Zhu, Z., Sun, J., Dong, S., 2019. Self-rechargeable-battery-driven device for simultaneous electrochromic windows, ROS biosensing, and energy storage. ACS Appl. Mater. Interfaces 11, 28072–28077. https://doi.org/10.1021/acsami.9b08715.
Zhai, Y., Li, J., Shen, S., Zhu, Z., Mao, S., Xiao, X., Zhu, C., Tang, J., Lu, X., Chen, J., 2022. Recent advances on dual-band electrochromic materials and devices. Adv. Funct. Mater. 32, 2109848. https://doi.org/10.1002/adfm.202109848.
Zhao, Z., Wang, M., Qiao, X., 2025. Electrochromic properties of nanostructured WO_3 thin films deposited on ITO/PET substrate modified by Pt sputtering. J. Phys. Conf. Ser. 2951, 012143. https://doi.org/10.1088/1742-6596/2951/1/012143.
Zheng, T., Zhang, H., Chen, C., Tu, X., Fang, L., Zhang, M., He, W., Wang, P., 2024. Self-powered dual-band electrochromic supercapacitor devices for smart window based on ternary dielectric triboelectric nanogenerator. Nanomaterials 14, 229. https://doi.org/10.3390/nano14020229.